Geophysical Research Letters

Supporting Information for

Satellite-based Estimation of Cloud-top Radiative Cooling Rate for Marine Stratocumulus

Youtong Zheng[1], Daniel Rosenfeld [2], Yannian Zhu [3], and Zhanqing Li[1]

[1]Earth System Science Interdisciplinary Center, University of Maryland, College Park, Maryland, 20742, USA.

[2] Institute of Earth Sciences, The Hebrew University of Jerusalem, Jerusalem, 91904, Israel.

[3] Meteorological Institute of Shaanxi Province, Xi'an, China

Contents of this file

1. Text S1 to S3
2. Table S1
3. Figures S1 to S6

Text S1: Radiative transfer model and the configuration

We use the Santa Barbara DISORT Atmospheric Radiative Transfer (SBDART) model [*Ricchiazzi et al.*, 1998]. The SBDART code ingests sophisticated discrete ordinate radiative transfer calculations and the atmospheric transmission models. It has been widely used in atmospheric researches. We specify the vertical grids with resolutions of 50 m from the surface to 2.25 km, 200 m from 2.25 km to 8 km, and 3 km from 8 km above. The surface type is set to "sea water". The ozone profile is set to default values for the tropical ocean. The input optical depth is uniformly distributed over the altitude range of the cloud layer. The SBDART was run twice for each case: the longwave run (5 ~ 40 μm) and the shortwave run (0.1 ~ 5 μm). The inclement of the wavelength range is set to 0.1 μm.

Text S2: Influence of H_t on CTRC

To illustrate the H_t influence on CTRC, we take the same example in Figure 1 and vary the satellite derived H_t from 1.0 to 1.5 km by varying the lapse rate from 9.7 to 6.5 K/km. Here, the T_t and SST are fixed, so their effects on CTRC are effectively controlled. Figure S4a-c shows the vertical profiles of temperature, moisture, and simulated heating rate for the six experiments with varied H_t. Figure S4d shows the sensitivity of the CTRC to the H_t. Only weak sensitivity (several W m^{-2}) is noted. Although the H_t differs by as large as 0.5 km (quadruples the mean error of satellite H_t retrieval, 0.13 km, as shown in Figure S1a), the radiative cooling values are close to the "ground truth" values marked by the black circles and triangles in Fig. S4d. Such an insensitivity arises from the fixation of T_t. On one hand, due to the fixed T_t, the cloud infrared emission remains unchanged. On the other hand, the water vapor mixing ratio at the cloud top also remains nearly unchanged because it is constrained by the T_t (Fig. S4b). Being most adjacent to the cloud top, the cloud-top moisture dominates the downwelling infrared radiation over the moisture loading in higher altitudes, leaving the downwelling infrared radiation vary little under the fixed-T_t condition.

There is a slight enhancement of CTRC with increased H_t. This is due to the free-tropospheric precipitable water decreasing with increased H_t (Fig. S4b). This mechanism can be used to interpret a potential cancellation of CTRC when the T_t is changed. For example, underestimation in T_t causes underestimation in CTRC via the weakened Planck function. However, a lower T_t gives a higher H_t, enhancing the CTRC and compensating for the underestimated CTRC.

Text S3: Error propagation analysis

Calculation of CTRC involves complicated radiative transfer equations, so it is not feasible to quantify the uncertainty mathematically. Following *Wood and Bretherton* [2004], we construct "erroneous" input by assigning estimated errors to each input parameter. This gives us "erroneous" CTRC, validating of which against the original CTRC gives us the root-mean-square error (RMSE) and bias for each input parameter. The overall error is calculated assuming random errors in all the input parameters. The result of the error propagation analysis is summarized in Table S1.

Aircraft measurements over the southeast Pacific shows that the satellite retrieved τ and r_e for closed-cell have RMSE of ~ 2 and ~2 μm, respectively *[Painemal and Zuidema,* 2011; *Witte et al.*, 2018]. At nighttime, because we assign climatological mean values to τ and r_e, we estimate the uncertainties to be 6 and 5 μm for τ and r_e, respectively, based on their climatological standard deviations from satellite data [*Chang et al*. 2007]. Note that the dependence of CTRC on τ is nonlinear: the dependence is strong in semi-transparent clouds and it saturates after τ reaches ~ 10 [*Zheng et al*., 2016]. So the potential error could be much larger than the estimation here for semi-transparent stratocumulus decks. For SST and T_t, we assign an error of 1K according to *Wood and Bretherton* [2004]. Our validation result (Fig. S1c) shows that the RMSE of reanalysis PW_{FA} is ~ 2mm (~ 30% percentage error). Here we use the percentage error, instead of RMSE, to construct the "erroneous" PW_{FA} because some cases have PW_{FA} < 2 mm and a minus PW_{FA} makes no physical sense. For the lapse rate of marine boundary layer, we assign an error of 1 K/km, which corresponds to 0.1~ 0.2 km error in H_t for typical marine boundary layers.

Table S1: Propagated bias and RMSE in $\Delta_{CT}F$ and $\Delta_{BL}F$ for estimated errors (second column) in each input parameter. The overall errors in bias and RMSE (last row) are calculated assuming random errors in all input parameters. The first and second value in the parenthesis of the last row represents the daytime and nighttime, respectively.

Input parameter		**Error**	**Δ_{CT}F (W m^{-2})**		**Δ_{BL}F (W m^{-2})**	
			Bias	RMSE	Bias	RMSE
τ	Daytime	±2	0.9	4.0	-1.4	4.3
	Nighttime	±6	5.3	11.6	0.0	4.5
r_e	Daytime	±2 µm	0.3	1.9	-1.7	3.8
	Nighttime	±5 µm	1.1	3.5	-2.3	3.9
SST		±1 K	0.1	4.5	-2.2	5.1
T_t		±1 K	0.0	4.4	-2.1	5.5
PW_{FA}		±2 mm (± 30%)	-0.5	6.9	-2.4	7.6
Lapse rate		±1 K/km	-0.5	4.5	-2.7	5.7
Overall error (W m^{-2})			0.5 (0.4/0.7)	5.7 (4.2/6.7)	-2.0 (-1.7/-2.3)	5.5 (4.8/6.0)

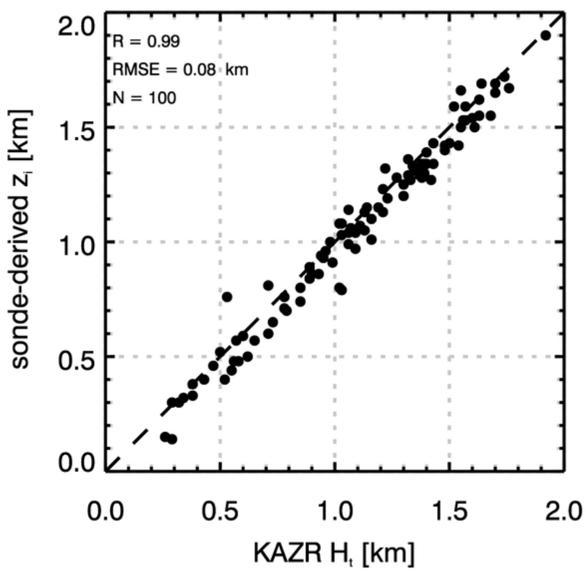

Figure S1: Comparison between the sonde-derived z_i and the KAZR-derived H_t. The H_t represents the three-hour average of the KAZR-measured cloud top heights. We use thresholds of signal-to-noise ratio of -13 and reflectivity of -40 dBZ to identify the cloudy pixels.

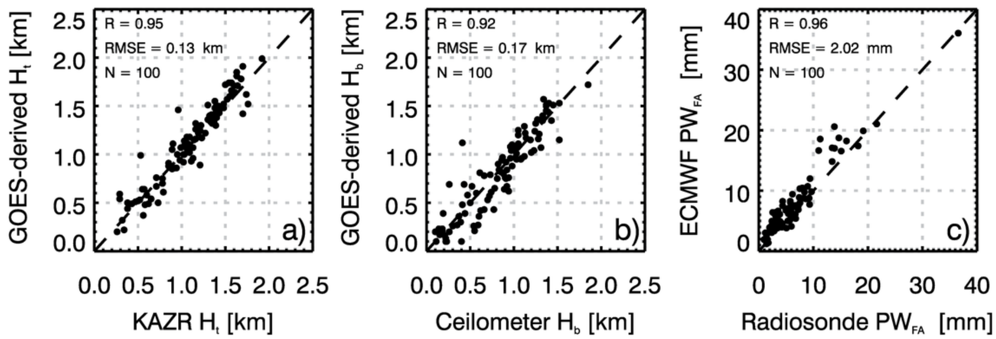

Figure S2: Comparisons between GOES-derived (a) H_t, (b) H_b, and (c) PW_{FA} against ARM ground-based measurements. The H_t and H_b are three-hour averages, measured from KAZR and ceilometer, respectively. Filled circles and upward triangles stand for daytime and nighttime cases, respectively.

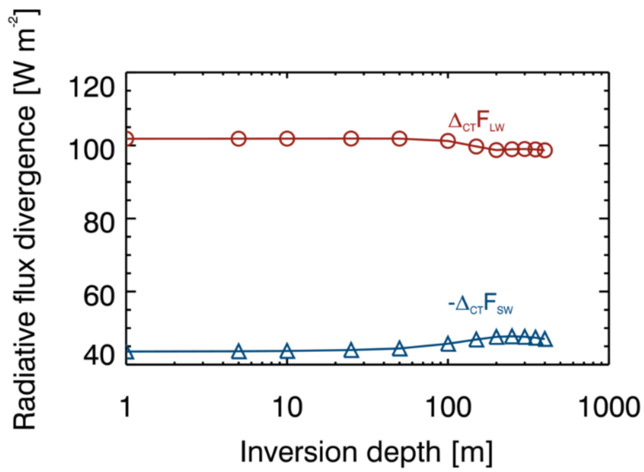

Figure S3: Sensitivity of the $\Delta_{CT}F_{LW}$ and $-\Delta_{CT}F_{SW}$ to the depth of the inversion capping the boundary layer for the composite mean case. Increase in inversion depth can increase the water vapor loading in the inversion layer, thus weakening the $\Delta_{CT}F_{LW}$ slightly. The more humid inversion-layer air absorbs additional shortwave radiation, increasing the $-\Delta_{CT}F_{SW}$ by just several W m^{-2}.

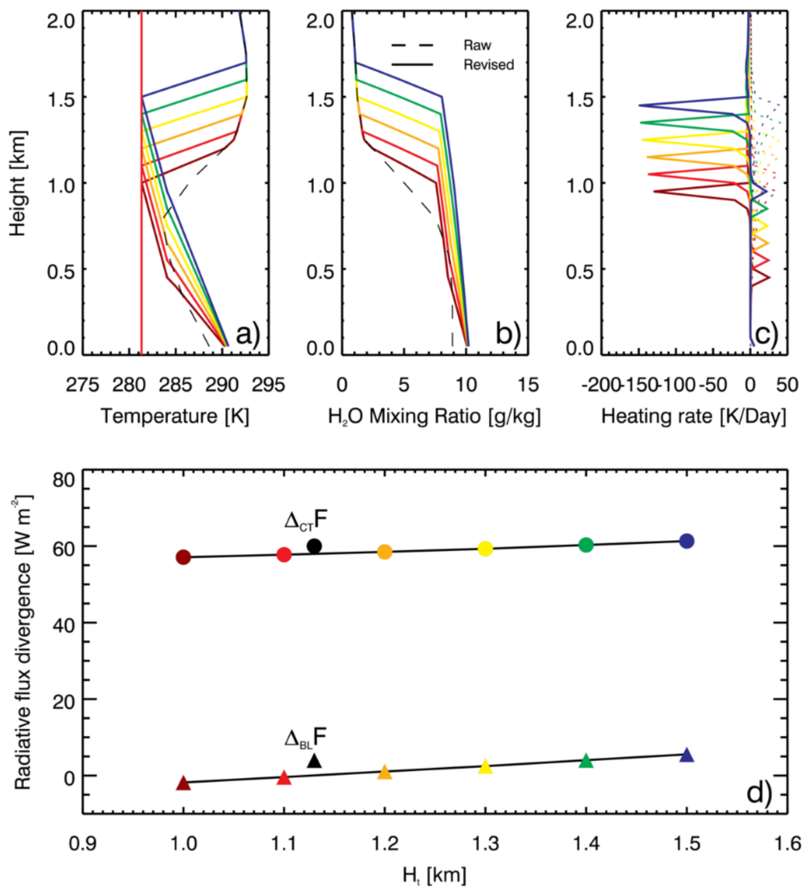

Figure S4: Vertical profiles of temperature (a), water vapor mixing ratio (b), and simulated longwave (solid) and shortwave (dotted) heating rate (c) for the six experiments with varied H_t. (d) Dependence of the $\Delta_{CT}F$ (filled circle) and $\Delta_{BL}F$ (filled upward triangle) with the H_t. The black symbols show the radiosonde-based estimations.

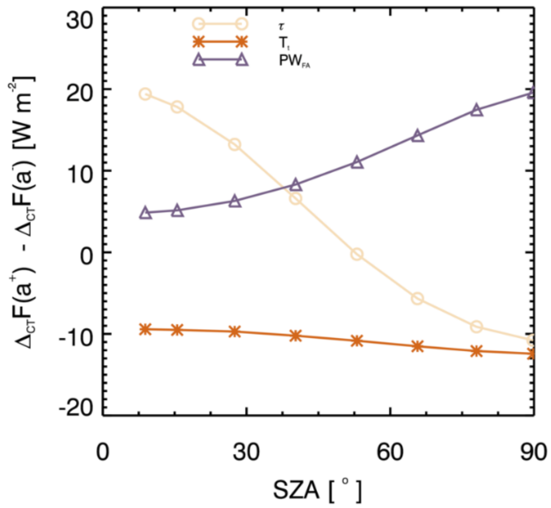

Figure S5: Variations of the $\Delta_{CT}F$ sensitivity to the three most influential input parameters with the solar zenith angle. In the y-axis, the *a* in the parenthesis refers to the input parameters and the superscript "+" and "-" refer to the 75th and 25th percentiles of the composite of each input parameter.

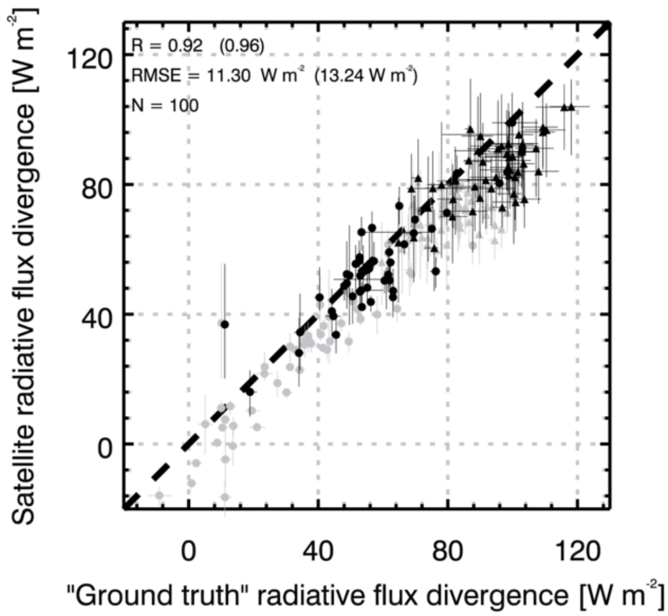

Figure S6: Same to Figure 3, but use NCEP/NCAR reanalysis instead of ECMWF.

Reference:

Chang, F. L., & Coakley Jr, J. A. (2007), Relationships between marine stratus cloud optical depth and temperature: Inferences from AVHRR observations. *Journal of Climate*, *20*(10), 2022-2036.

Painemal, D., and P. Zuidema (2011), Assessment of MODIS cloud effective radius and optical thickness retrievals over the Southeast Pacific with VOCALS-REx in situ measurements, *Journal of Geophysical Research: Atmospheres*, *116*(D24).

Ricchiazzi, P., S. Yang, C. Gautier, and D. Sowle (1998), SBDART: A research and teaching software tool for plane-parallel radiative transfer in the Earth's atmosphere, *B Am Meteorol Soc*, *79*(10), 2101-2114.

Witte, M. K., Yuan, T., Chuang, P. Y., Platnick, S., Meyer, K. G., Wind, G., & Jonsson, H. H. (2018), MODIS retrievals of cloud effective radius in marine stratocumulus exhibit no significant bias. *Geophysical Research Letters*, *45*(19), 10-656.

Wood, R., & Bretherton, C. S. (2004), Boundary layer depth, entrainment, and decoupling in the cloud-capped subtropical and tropical marine boundary layer. *Journal of Climate*, *17*(18), 3576-3588.

Zheng, Y., Rosenfeld, D., & Li, Z. (2016). Quantifying cloud base updraft speeds of marine stratocumulus from cloud top radiative cooling. *Geophysical Research Letters*, *43*(21), 11-407.